buildings

MDPI

*Article*

# Study on Shock-Absorbing Effect of a Double-Story Isolation Structure Considering Soil–Structure Interaction

**Liang Gao [1], Dewen Liu [1,*], Min Lei [2], Yong Ding [1] and Shian Mu [1]**

[1] College of Civil Engineering, Southwest Forestry University, Kunming 650000, China; gaoliang1331@sina.com (L.G.); civil-dingyong@foxmail.com (Y.D.); mushian2019@163.com (S.M.)
[2] College of Civil Engineering, Southwest Jiaotong University, Chengdu 610000, China; xnjdleimin@163.com
* Correspondence: civil_liudewen@sina.com

**Abstract:** The double-story isolation structure is a novel development based on the mid-story isolation structure. To accurately reflect the seismic response of the double-story isolation structure, this study considers a dynamic elastoplastic analysis model that incorporates soil–structure interaction (SSI). Comparative models of a base-fixed structure and a mid-story isolation structure are also established. The results indicate that the double-story isolation structure has a longer structural period compared to the mid-story isolation structure. Furthermore, the structural period increases as the soil softens and the structure becomes more flexible. When considering SSI on hard soil versus not considering SSI, the double-story isolation structure exhibits smaller base shear, story force, inter-story displacement, maximum acceleration of the top floor, and displacement of the upper isolation layer, indicating the significant shock-absorbing effect of the double-story isolation structure. However, when SSI is considered on soft soil, the shock-absorbing effect of the isolation structure diminishes, and the effectiveness of the double-story isolation structure may not necessarily surpass that of the mid-story isolation structure. In all three soil conditions, the compressive stresses of the isolation bearings in the upper isolation layer of the double-story isolation structure were lower than those in the isolation bearings of the base isolation layer. Additionally, the double-story isolation structure demonstrates reduced compressive stress in the isolation bearings, fewer plastic hinges in the frame, and less stress damage compared to the mid-story isolation structure. Consequently, the risk of overturning damage in the double-story isolation structure is significantly reduced compared to the mid-story isolation structure. The effect of soft ground on structures can be highly detrimental, which should be paid more attention to during the design process. This study offers valuable insights for future research on double-story isolation systems and serves as a reference for the development of high-performance building structures in the future.

**Keywords:** double-story isolation structure; mid-story isolation structure; soil–structure interaction; seismic response



**Citation:** Gao, L.; Liu, D.; Lei, M.; Ding, Y.; Mu, S. Study on Shock-Absorbing Effect of a Double-Story Isolation Structure Considering Soil–Structure Interaction. *Buildings* **2023**, *13*, 2677. https://doi.org/10.3390/buildings13112677

Academic Editor: Piero Colajanni

Received: 8 September 2023
Revised: 13 October 2023
Accepted: 20 October 2023
Published: 24 October 2023



## 1. Introduction

Earthquakes have consistently been devastating natural disasters, causing significant economic losses worldwide and posing a grave threat to the safety of countless individuals. The development of high-performance structures capable of withstanding earthquakes has long been a paramount concern for people worldwide. In recent years, seismic isolation technology has experienced rapid development and extensive utilization in practical engineering. The double-story isolation system is a novel type of isolation system developed from the mid-story isolation system. A double-layered isolation structure consists of two isolation layers, each equipped with seismic isolators. The comparative diagram of different structures is illustrated in Figure 1. Ancient architecture also features a similar structure, as depicted in Figures 2 and 3. The structure is divided into multiple interconnected substructures using damping mechanisms. This configuration allows for the

dissipation of seismic energy among the substructures, effectively minimizing structural damage. Chai [1] proposed an isolation method, which was an early theoretical system for double-story isolation structures. The double-story isolation structure not only reduces the seismic response but also enhances the overturning resistance of the structure [2].

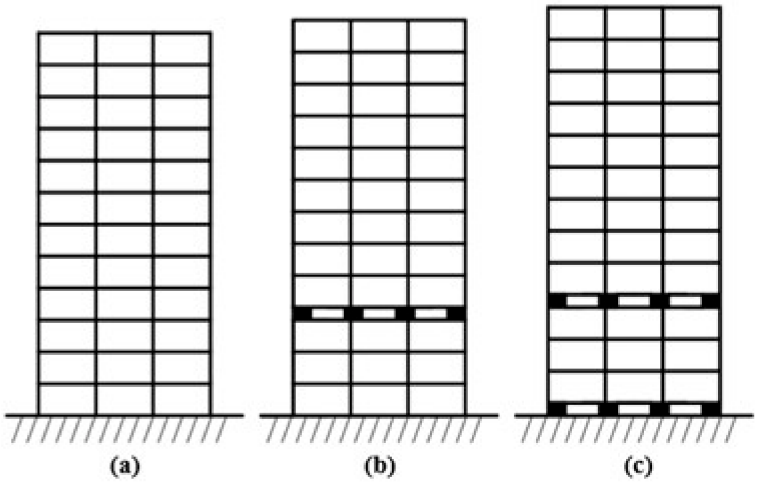


**Figure 1.** Comparison diagram of different structures. (**a**) Base-fixed structure; (**b**) Mid-story isolation structure; (**c**) Double-story isolation structure.

**Figure 2.** The Parthenon in Greece.

**Figure 3.** Dharani Sutra Pillar in Zhaozhou, China.

The majority of current research on seismic isolation primarily focuses on conventional isolation structures, which have already made significant advancements in terms of research theory. Loh et al. [3] conducted a study that examined the time-varying dynamic characteristics of a mid-story isolation building by utilizing both ambient vibration test data and earthquake response data. Zhou et al. [4] introduced an approach based on modal synthesis to create a reduced model of the second, third, or higher order for representing the structure of a mid-story isolation building. Takewaki et al. [5] compared a base isolation structure equipped with a viscous damper to another structure equipped with an elastic plastic hysteretic damper. Eem and Jung [6,7] introduced the concept of the stochastic response database to obtain the instantaneous seismic response distributions of an isolation structure and evaluated the seismic fragility of an isolation structure. Fallahian et al. [8] examined the reactions of a torsionally coupled base isolation structure, which was supported by triple concave friction pendulum bearings (TFP), when subjected to near-field ground motions. Yang et al. [9] conducted a study on the structural robustness of various vertical irregular isolation structures under different earthquakes. Zhu et al. [10] conducted a three-dimensional nonlinear dynamic time analysis of a house model and compared it with a shaking table model. Wu and Li [11] conducted an analysis of the impact of vertical ground vibration on the limits of height-to-width ratio in rubber bearing isolation structures. Pan et al. [12] conducted a comparative analysis of the seismic susceptibility of a large span-shaped steel corridor continuous structure with a base isolation and non-isolation continuous structure. Zhang et al. [13] introduced the concept of energy spectrum for design and developed a prediction equation for the seismic response of a laminated mid-story isolation structure based on energy balance. Shi et al. [14] assessed the predominant collapse mode of isolated structures exposed to multidirectional dynamic coupling excitations using reliability theory. Wang and Huang [15] introduced an approach for seismic reliability analysis that relies on a global damage model applied to a base isolation structure.

Isolation structures are typically constructed on soil, and the interaction between the soil and the structure is objectively evident during an earthquake. Karabork et al. [16] investigated the impact of soil–structure interaction on the response of a base isolation structure. Ashiquzzaman and Hong [17] highlighted the substantial influence of soil–structure interaction on the seismic isolation of containment buildings within a nuclear power plant during extremely intense ground motion events. Shourestani et al. [18] investigated the effects of soil–structure interaction on the seismic performance of a smart base isolation structure. Krishnamoorthy [19] investigated the influence of soil–structure interaction on the seismic response of a multi-degree-of-freedom isolation structure equipped with a friction pendulum system. Zhang et al. [20] demonstrated the damping properties of a soil–structure interaction system by conducting a shaking table experiment. Liu et al. [21] examined the effectiveness of vibration control using an eddy current tuned mass damper on a structure while considering soil–structure interaction under seismic loading conditions. Dong et al. [22] examined the seismic performance of a self-centering rocking bent, considering the impact of soil–structure interaction.

Currently, there is limited research on double-story isolation structure systems. Zhang et al. [23] demonstrated that a segmented isolation structure can reduce the likelihood of tensile or shear damage to the isolation bearing by utilizing a two-mass model. Rong et al. [24,25] conducted a study on the seismic response of double-story isolation structures under both ordinary ground motion and near-fault ground motion conditions, considering different positions for the upper isolation layer. Their findings indicated that optimal seismic isolation performance is achieved when the upper isolation layer is positioned in the middle and lower part of the structure. Ou et al. [2] conducted shaking table tests to examine double-story isolation structures, which demonstrated excellent resistance to overturning. However, these studies made the simplifying assumption of a rigid foundation and did not account for soil–structure interaction, which imposes certain limitations on their applicability. Based on the previous study, in this research, the upper isolation layer is

positioned on the third layer of the double-story isolation structure. The base-fixed model, mid-story isolation model, and double-layer isolation model are established to analyze the seismic response while considering soil–structure interaction (SSI). It provides insights for further research on double-story isolation systems and serves as a reference for the development of future high-performance building structures.

## 2. Structural Model

### *2.1. Overview*

The building is a 12-story frame structure, the floor height is 3 m, and the building plane size is 13.5 m × 32.5 m. The design basic acceleration of ground motion is 0.2 g, the site category is Class II, and the seismic design grouping is Group II. The column size is 800 mm × 800 mm, the size of main beam is 700 mm × 300 mm, the size of secondary beam is 600 mm × 300 mm. The concrete strength grade of the frame columns is C40, while the concrete strength grade of the beams is C30. The slab thickness is 150 mm. The longitudinal reinforcement type is HRB400, and the stirrup type is HPB300. The thickness of the concrete protective layer is 40 mm. A 3D view of the structure is shown in Figure 4.

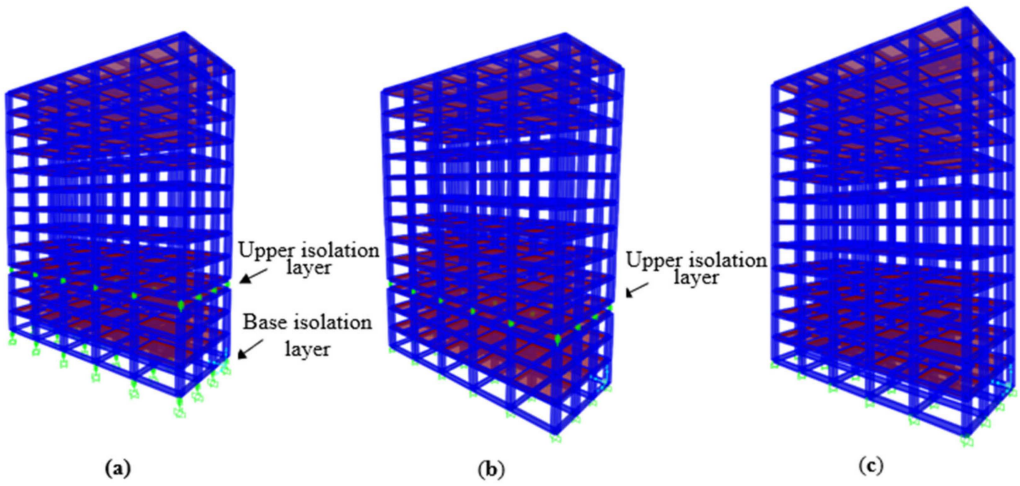


**Figure 4.** A 3D view of the structure. (**a**) Double-story isolation structure; (**b**) Mid-story isolation structure; (**c**) Base-fixed structure.

### *2.2. Model Building*

The finite element software SAP2000 (v24.0.0) was used to establish the base-fixed structure model, mid-story isolation structure model, and double-story isolation structure model. The mid-story isolation structure incorporates an upper isolation layer positioned at the third layer. The double-story isolation structure consists of a base isolation layer located at the bottom of the structure and an upper isolation layer positioned at the third layer. Elastoplastic time history analysis was conducted for the base-fixed structure, mid-story isolation structure, and double-layer isolation structure. The selected solution method utilizes direct integration with a time step of 0.02. The total number of time steps is calculated by dividing the total duration of seismic waves by the time step. The lead-core rubber isolation bearings (LRB600) were arranged in the isolation layer. The parameters of the isolation bearings are shown in Table 1, and the layout of the isolation bearings is shown in Figure 5. Rubber isolator units are used for the isolation bearings. Takeda hysteresis type is used for C40 concrete, and kinematic hysteresis type is used for both HPB300 and HRB400 reinforcements. The Takeda hysteresis curve is depicted in Figure 6, while the kinematic hysteresis curve is displayed in Figure 7. P-M2-M3 fiber hinges are used for the frame columns, and M3 hinges are used at both ends for the frame beams and secondary beams.

**Table 1.** Parameters of the isolation bearings.

| Type | Effective Diameter (mm) | Total Rubber Thickness (mm) | Stiffness Before Yield (kN/m) | 100% Horizontal Shear Deformation (kN/m) | 250% Horizontal Shear Deformation (kN/m) | Vertical Stiffness (kN/mm) | Yield Force (kN) |
|---|---|---|---|---|---|---|---|
| LRB600 | 600 | 110 | 13,110 | 1580 | 1580 | 2800 | 63 |

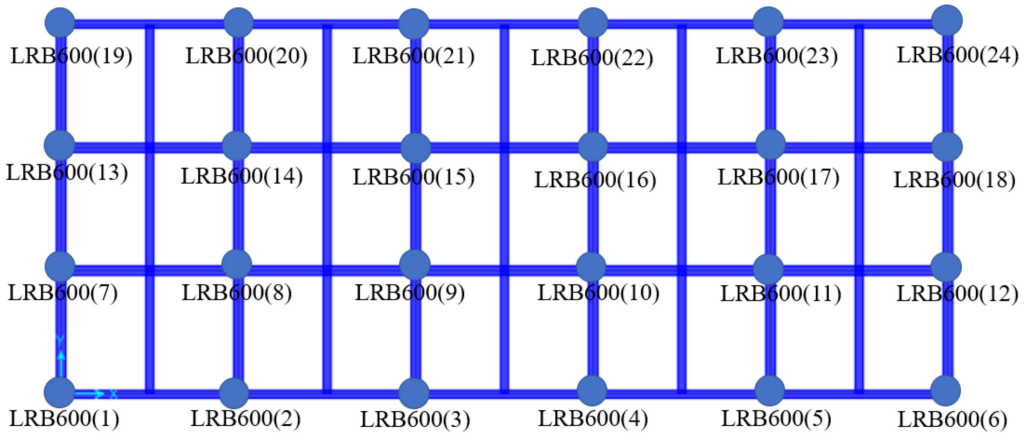


**Figure 5.** Layout of the isolation bearings.

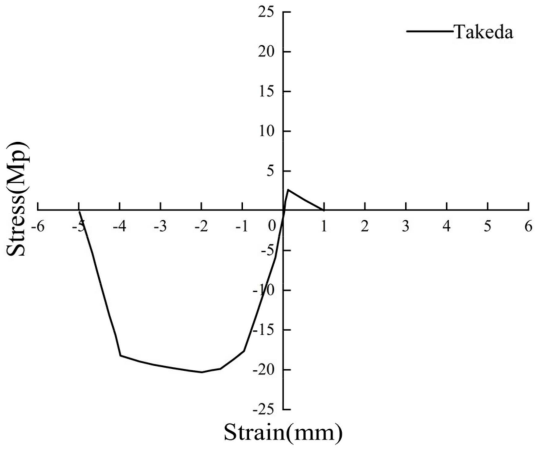


**Figure 6.** Takeda hysteresis curve.

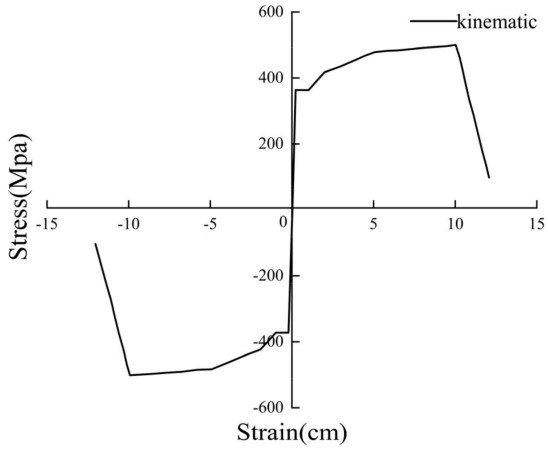


**Figure 7.** Kinematic hysteresis curve.

### *2.3. Seismic Wave Selection*

The seismic intensity of the area is of the 8th degree. Three seismic waves were selected from the Pacific Earthquake Engineering Research Center. The basic information of ground motions is shown in Table 2. The earthquake response spectrum is shown in Figure 8. According to the Code for Seismic Design of Buildings [26], the average base shear value of the structure calculated from multiple time curves should not be less than 80% of the result obtained from the design response spectrum method. The calculated results of seismic waves are shown in Table 3. The peak acceleration of the seismic wave was set to 400 cm/s$^2$, which corresponds to the peak acceleration associated with the 8th degree during rare earthquakes.

**Table 2.** Basic information of ground motions.

| Earthquake | Year | Station | Magnitude | Fault Distance (km) | PGV (cm/s) | PGA (cm/s$^2$) | PGV/PGA |
|---|---|---|---|---|---|---|---|
| Kern County wave | 1952 | Taft Lincoln School | 7.36 | 38.42 | 15.2 | 155.7 | 0.10 |
| Whittier Narrows wave | 1987 | Santa Monica—Second St | 5.99 | 32.8 | 3.0 | 33.4 | 0.09 |
| Chi-Chi wave | 1999 | KAU054 | 7.62 | 27.37 | 7.6 | 84.1 | 0.09 |

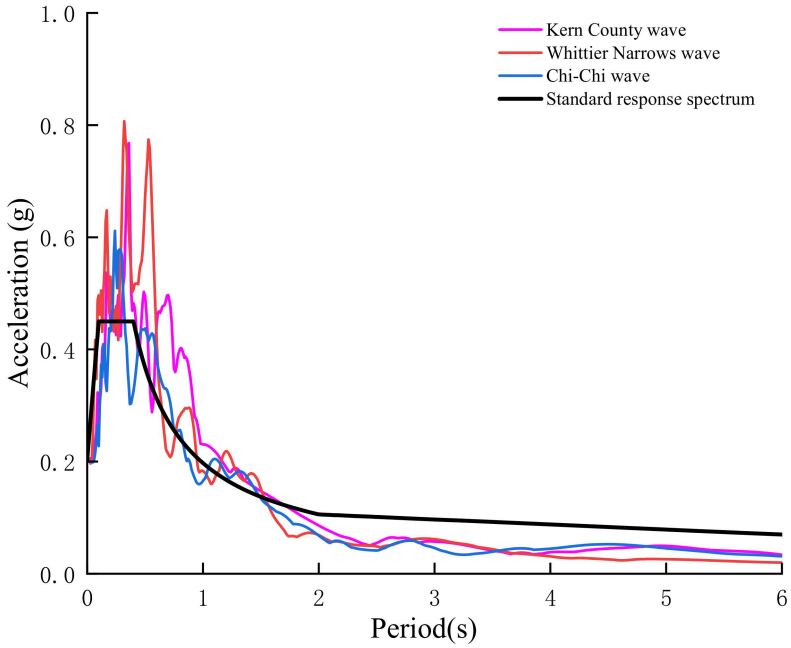


**Figure 8.** Earthquake response spectrum.

**Table 3.** Calculated results of seismic wave.

| Condition | Base Shear (kN) | Time History/Response Spectrum |
|---|---|---|
| Response spectrum | 12,366 | / |
| Kern County | 10,568 | 85.46% |
| Whittier Narrows | 10,063 | 81.38% |
| Chi-Chi | 11,083 | 89.62% |
| Average value | 10,571 | 85.48% |

## 3. Implementation of SSI

The independent bases under columns are used for the base-fixed structure, mid-story isolation structure, and double-story isolation structure, with base sizes of 4 m × 4 m, a thickness of 1 m, and a base burial depth of 3.5 m. The methods proposed by ATC40

and FEMA440 [27,28] were employed to model soil–structure interaction. The simplified model is shown in Figure 9, the stiffness of the simplified model is shown in Table 4, and the parameters of different soils are shown in Table 5.

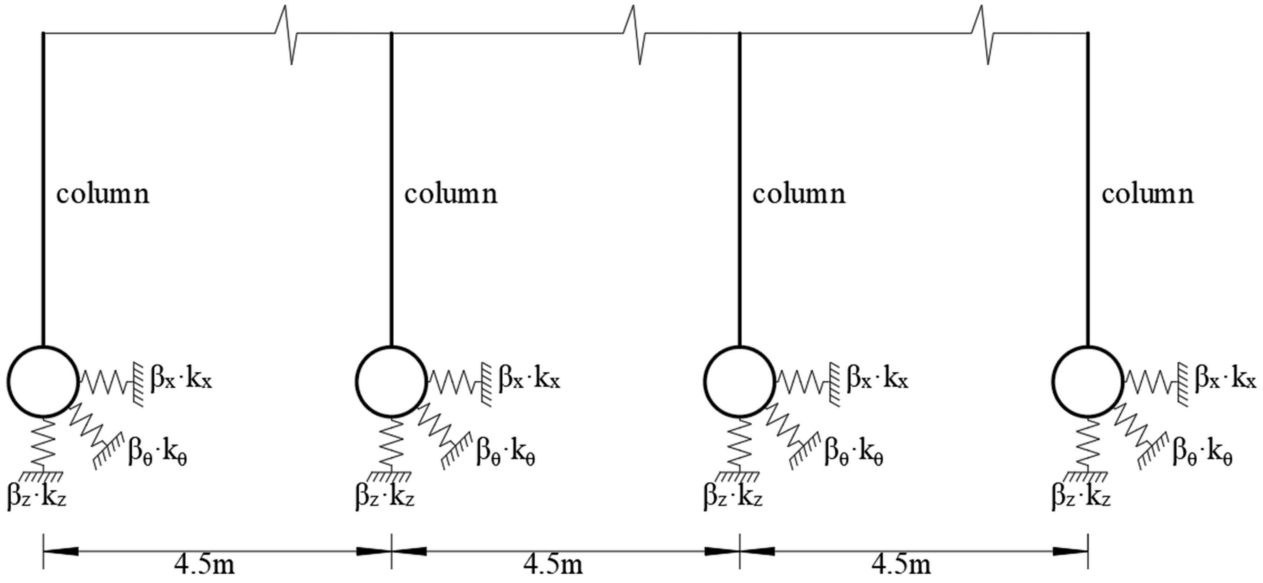


**Figure 9.** Soil spring model (the short side of the structural plane).

**Table 4.** Stiffness formulae and their corresponding embedment factors of soil spring.

| Mode | Stiffness Coefficient | Embedment Factor $\beta_z$ |
|---|---|---|
| Vertical stiffness $k_z$ | $\frac{GL}{1-\nu}\left[0.73+1.54\left(\frac{B}{L}\right)^{0.75}\right]$ | $\left[1+0.095\frac{D}{B}\left(1+1.3\frac{B}{L}\right)\right]\left[1+0.2\left(\frac{(2L+2B)}{LB}d\right)^{0.67}\right]$ |
| Horizontal y-directional stiffness $k_y$ | $\frac{GL}{2-\nu}\left[2+2.5\left(\frac{B}{L}\right)^{0.85}\right]$ | $\left[1+0.15\left(\frac{2D}{B}\right)^{0.5}\right]\left[1+0.52\left[\frac{16(D-d/2)(L+B)}{BL^2}d\right]^{0.4}\right]$ |
| Horizontal x-directional stiffness $k_x$ | $\frac{GL}{2-\nu}\left[2+2.5\left(\frac{B}{L}\right)^{0.85}\right]-\frac{\mathrm{GL}}{0.75-\nu}\left[0.1\left(1-\frac{B}{L}\right)\right]$ | $\left[1+0.15\left(\frac{2D}{B}\right)^{0.5}\right]\left[1+0.52\left[\frac{16(D-d/2)(L+B)}{BL^2}d\right]^{0.4}\right]$ |
| Rotational stiffness $k_{\theta x}$ | $\frac{GL}{1-v}I_x^{0.75}\left(\frac{L}{B}\right)^{0.75}\left[2.4+0.5\frac{B}{L}\right]$ | $1+2.52\frac{d}{B}\left(1+\frac{2d}{B}\left(\frac{d}{D}\right)^{-0.2}\left(\frac{B}{L}\right)^{0.85}\right)$ |
| Rotational stiffness $k_{\theta y}$ | $\frac{GL}{1-v}I_y^{0.75}\left[3\left(\frac{B}{L}\right)^{0.15}\right]$ | $1+0.92\left(\frac{2d}{L}\right)^{0.6}\left[1.5+\left(\frac{2d}{L}\right)^{1.9}\left(\frac{d}{D}\right)^{-0.6}\right]$ |

Note: $G$ is the effective shear modulus; $\nu$ is the Poisson's ratio; $L$ is the length of the base; $B$ is the width of the base; $D$ is the burial depth of the base; $d$ is the thickness of the base. $I_x$ and $I_y$ are the sectional moments of inertia around the relevant axis, respectively.

**Table 5.** Soil parameters.

| Type | Shear Wave Velocity ($\mathbf{m \cdot s^{-1}}$) | Density | Poisson's Ratio | Initial Shear Modulus $G_0$ ($\mathbf{10^4\ kN \cdot m^{-2}}$) | Effective Shear Modulus $G = 0.42G_0$ ($\mathbf{10^4\ kN \cdot m^{-2}}$) | Cohesive Force | Angle of Internal Friction (°) |
|---|---|---|---|---|---|---|---|
| Soft soil | 150 | 1600 | 0.3 | 1.1 | 0.462 | 18 | 6 |
| Hard soil | 400 | 2000 | 0.2 | 12.4 | 5.208 | 47 | 28 |

## 4. Response Study of the Double-Story Isolation System with SSI

### *4.1. Comparison of Structural Periods*

The structural periods for different types of soil action are displayed in Tables 6–8. The natural period of vibration increases when an isolation layer is provided. A double-story isolation structure can extend the natural period of vibration even more compared to a

mid-story isolation structure, moving it farther away from the characteristic period of the site and thereby reducing the risk of structural damage. Considering SSI on hard soil, the period of the structure is greater than without SSI. Conversely, the period of the structure is at its highest when SSI is considered on soft soil.

**Table 6.** Base-fixed structure of structural periods and modal participating mass ratios.

| Type | Mode Number | Structural Periods (s) | Modal Participating Mass Ratios | | | | | |
|---|---|---|---|---|---|---|---|---|
| | | | Ux | Uy | Uz | Rx | Ry | Rz |
| Without SSI | 1 | 1.29 | 0.79 | 0 | 0 | 0 | 0.14 | 0 |
| | 2 | 1.18 | 0 | 0.78 | 0 | 0.22 | 0 | 0 |
| | 3 | 1.07 | 0 | 0 | 0 | 0 | 0 | 0.79 |
| | 4 | 0.41 | 0.10 | 0 | 0 | 0 | 0.29 | 0 |
| | 5 | 0.38 | 0 | 0.11 | 0 | 0.44 | 0 | 0 |
| | 6 | 0.34 | 0 | 0 | 0 | 0 | 0 | 0.10 |
| Considering SSI on soft soil | 1 | 2.55 | 0 | 0.77 | 0 | 0.23 | 0 | 0 |
| | 2 | 1.77 | 0.80 | 0 | 0 | 0 | 0.17 | 0 |
| | 3 | 1.46 | 0 | 0 | 0 | 0 | 0 | 0.82 |
| | 4 | 0.49 | 0.14 | 0 | 0 | 0 | 0.59 | 0 |
| | 5 | 0.48 | 0 | 0 | 0.99 | 0 | 0 | 0 |
| | 6 | 0.46 | 0 | 0.18 | 0 | 0.61 | 0 | 0 |
| Considering SSI on hard soil | 1 | 1.39 | 0 | 0.78 | 0 | 0.21 | 0 | 0 |
| | 2 | 1.37 | 0.79 | 0 | 0 | 0 | 0.13 | 0 |
| | 3 | 1.17 | 0 | 0 | 0 | 0 | 0 | 0.78 |
| | 4 | 0.43 | 0.10 | 0 | 0 | 0 | 0.32 | 0 |
| | 5 | 0.39 | 0 | 0.12 | 0 | 0.47 | 0 | 0 |
| | 6 | 0.36 | 0 | 0 | 0 | 0 | 0 | 0.11 |

**Table 7.** Mid-story isolation structure of structural periods and modal participating mass ratios.

| Type | Mode Number | Structural Periods (s) | Modal Participating Mass Ratios | | | | | |
|---|---|---|---|---|---|---|---|---|
| | | | Ux | Uy | Uz | Rx | Ry | Rz |
| Without SSI | 1 | 2.83 | 0.78 | 0 | 0 | 0 | 0.10 | 0 |
| | 2 | 2.79 | 0 | 0.78 | 0 | 0.15 | 0 | 0 |
| | 3 | 2.52 | 0 | 0 | 0 | 0 | 0 | 0.78 |
| | 4 | 0.51 | 0 | 0 | 0 | 0 | 0.29 | 0 |
| | 5 | 0.48 | 0 | 0 | 0 | 0.42 | 0 | 0 |
| | 6 | 0.43 | 0 | 0 | 0 | 0 | 0 | 0 |
| Considering SSI on soft soil | 1 | 3.62 | 0 | 0.78 | 0 | 0.18 | 0 | 0 |
| | 2 | 3.08 | 0.79 | 0 | 0 | 0 | 0.11 | 0 |
| | 3 | 2.71 | 0 | 0 | 0 | 0 | 0 | 0.79 |
| | 4 | 0.75 | 0 | 0.01 | 0 | 0.27 | 0 | 0 |
| | 5 | 0.63 | 0 | 0 | 0 | 0 | 0.46 | 0 |
| | 6 | 0.49 | 0 | 0 | 0 | 0 | 0 | 0 |
| Considering SSI on hard soil | 1 | 2.88 | 0 | 0.77 | 0 | 0.14 | 0 | 0 |
| | 2 | 2.87 | 0.77 | 0 | 0 | 0 | 0.09 | 0 |
| | 3 | 2.57 | 0 | 0 | 0 | 0 | 0 | 0.77 |
| | 4 | 0.53 | 0 | 0 | 0 | 0.38 | 0 | 0 |
| | 5 | 0.52 | 0.01 | 0 | 0 | 0 | 0.30 | 0 |
| | 6 | 0.44 | 0 | 0 | 0 | 0 | 0 | 0 |

**Table 8.** Double-story isolation structure of structural periods and modal participating mass ratios.

| Type | Mode Number | Structural Periods (s) | Modal Participating Mass Ratios | | | | | |
|---|---|---|---|---|---|---|---|---|
| | | | Ux | Uy | Uz | Rx | Ry | Rz |
| Without SSI | 1 | 3.99 | 0.94 | 0 | 0 | 0 | 0.02 | 0 |
| | 2 | 3.96 | 0 | 0.94 | 0 | 0.03 | 0 | 0 |
| | 3 | 3.58 | 0 | 0 | 0 | 0 | 0 | 0.94 |
| | 4 | 1.04 | 0.06 | 0 | 0 | 0 | 0.40 | 0 |
| | 5 | 1.04 | 0 | 0.06 | 0 | 0.58 | 0 | 0 |
| | 6 | 0.93 | 0 | 0 | 0 | 0 | 0 | 0.06 |
| Considering SSI on soft soil | 1 | 4.64 | 0 | 0.92 | 0 | 0.07 | 0 | 0 |
| | 2 | 4.18 | 0.94 | 0 | 0 | 0 | 0.03 | 0 |
| | 3 | 3.72 | 0 | 0 | 0 | 0 | 0 | 0.94 |
| | 4 | 1.15 | 0 | 0.08 | 0 | 0.83 | 0 | 0 |
| | 5 | 1.08 | 0.06 | 0 | 0 | 0 | 0.51 | 0 |
| | 6 | 0.95 | 0 | 0 | 0 | 0 | 0 | 0.06 |
| Considering SSI on hard soil | 1 | 4.03 | 0 | 0.94 | 0 | 0.04 | 0 | 0 |
| | 2 | 4.01 | 0.94 | 0 | 0 | 0 | 0.02 | 0 |
| | 3 | 3.61 | 0 | 0 | 0 | 0 | 0 | 0.94 |
| | 4 | 1.05 | 0 | 0.06 | 0 | 0.61 | 0 | 0 |
| | 5 | 1.05 | 0.06 | 0 | 0 | 0 | 0.41 | 0 |
| | 6 | 0.93 | 0 | 0 | 0 | 0 | 0 | 0.06 |

The SSI effect has a more significant impact on the first-order modes of structures and a lesser influence on the higher-order modes. Specifically, it has the greatest influence on base-fixed structures and the least impact on double-story isolation structures. A double-story isolation structure minimizes the impact of various soil types on the structural response. The first- and second-order modes of all three structures primarily exhibit translational motion, while torsional motion mainly occurs in the third-order mode. Additionally, translational and torsional motions exhibit limited distribution among the higher-order modes. When accounting for the SSI effect, the structural stiffness softens, resulting in a more flexible structure with an extended period.

### *4.2. Comparison of Base Shear*

The base shear for the different structures is shown in Figure 10. In all three soil cases, the base shear of the fixed foundation structure exceeds that of the mid-story isolation structure, while the base shear of the double-story isolation structure is the smallest. This indicates the remarkable ability of the double-story isolation structure to effectively reduce the base shear and provide an excellent shock-absorbing effect. However, when considering SSI, the base shear of the double-story isolation structure on hard soil is slightly greater than the base shear without SSI. On the other hand, the base shear of the double-story isolation structure with SSI on soft soil is the greatest.

The SSI effect has a more significant impact on base-fixed structures. Considering the SSI effect results in a higher base shear in double-story isolation structures and mid-story isolation structures. Furthermore, accounting for the SSI effect leads to a greater variation in the base shear produced by base-fixed structures.

### *4.3. Comparison of Inter-Story Displacement*

The inter-story displacements of the structure with different soil properties are presented in Figure 11. According to the Code for Seismic Design of Buildings [26], the inter-story displacement in this paper cannot exceed 33 mm. None of the structures exceed the normative limit value. The inter-story displacements of the double-story isolation structure without SSI are lower than those when considering SSI on hard soil. However, the inter-story displacements are highest when SSI is considered in soft soil. Comparatively, the double-story isolation structure exhibits smaller inter-story displacement than the

mid-story isolation structure, both without SSI and when considering SSI on hard soil. The double-story isolation structure demonstrates effective control over floor displacements and exhibits superior seismic isolation capacity both when SSI is not considered and when considering SSI on hard soil.

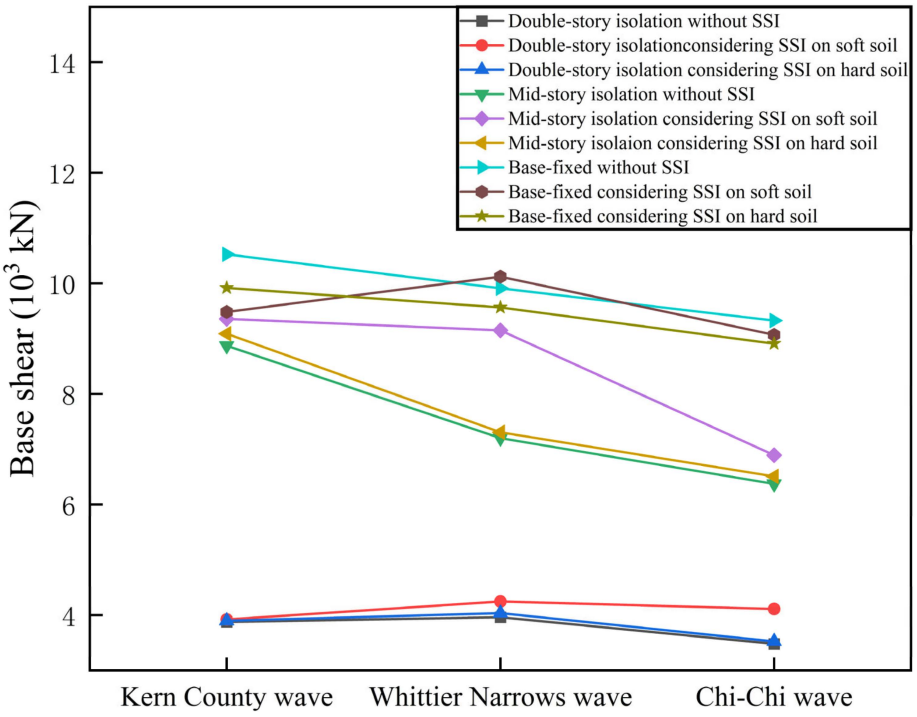


**Figure 10.** Comparison of base shear.

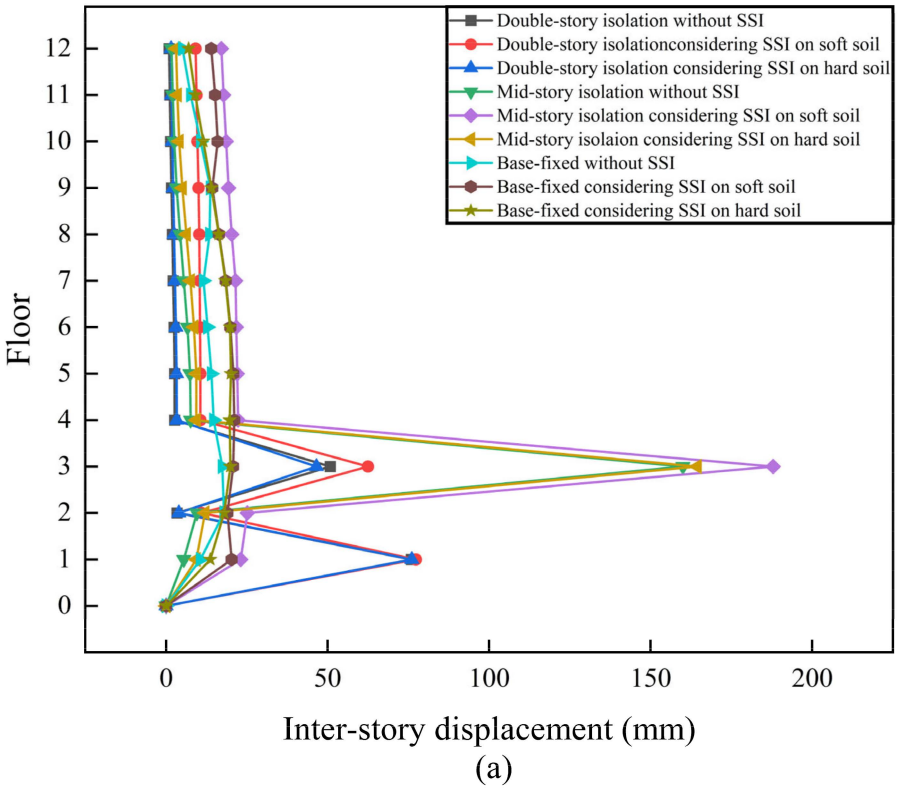


**Figure 11.** *Cont.*

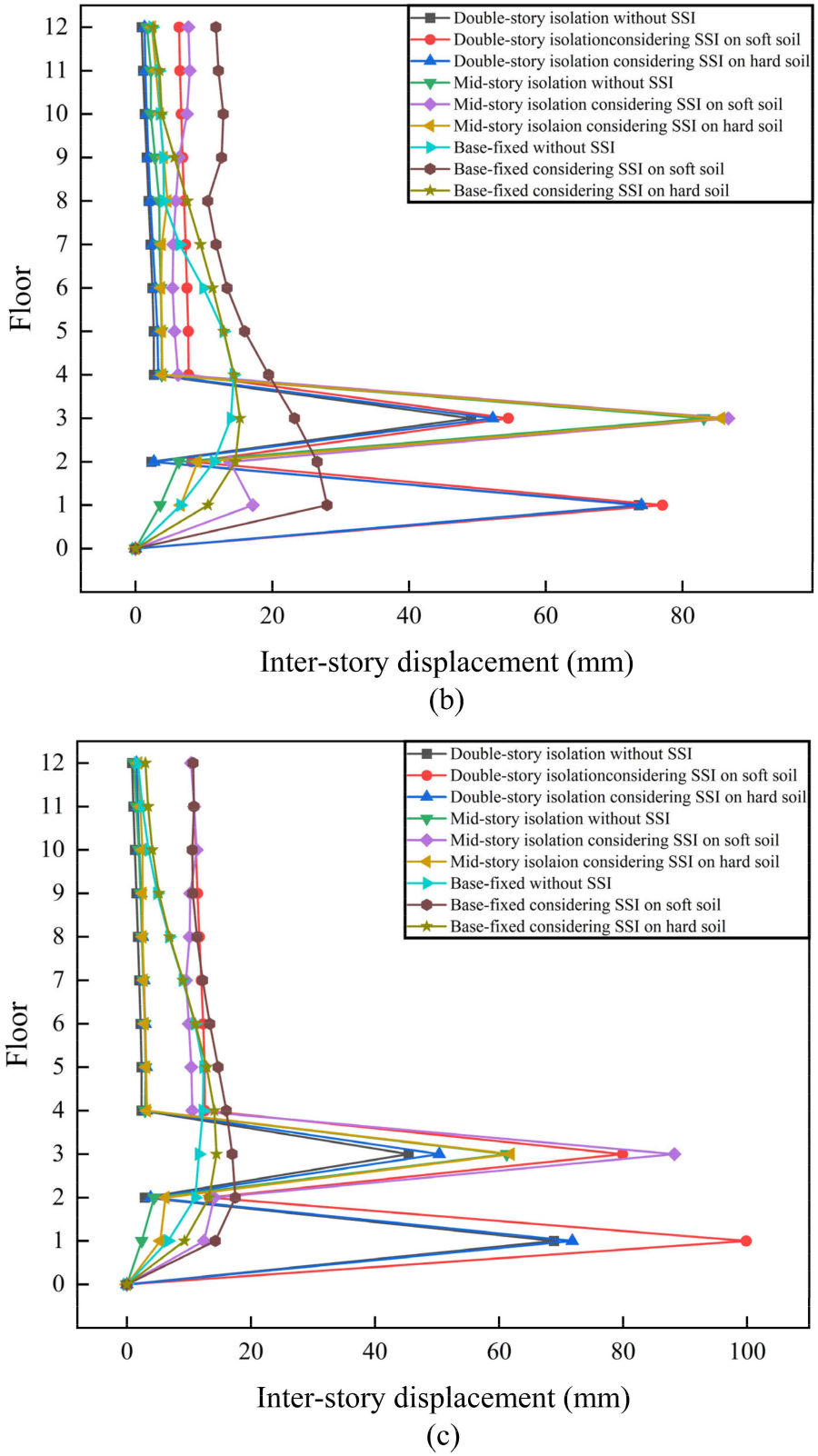


**Figure 11.** Inter-story displacement of the structure. (**a**) Inter-story displacement under the action of Kern County wave; (**b**) Inter-story displacement under the action of Whittier Narrows wave; (**c**) Inter-story displacement under the action of Chi-Chi wave.

When considering SSI on soft soil, the inter-story displacements of the structure become more complex. Double-story isolation structures, mid-story isolation structures,

and base-fixed structures exhibit varying inter-story displacements under the influence of different seismic waves. It is crucial to note that on soft foundations, the seismic damping effect of isolation structures is poor, sometimes even surpassing the seismic response observed without isolation. Therefore, greater attention should be devoted to the design of buildings constructed on soft foundations.

### *4.4. Comparison of Story Shear*

The floor shear of the structure under various soil conditions is illustrated in Figure 12. When considering SSI on hard soil, the floor shear of the double-story isolation structure is higher compared to cases without SSI. Additionally, the floor shear is greatest when SSI is considered on soft soil. Without SSI and with SSI on hard soil, the mid-story isolation structure exhibits lower floor shear compared to the base-fixed structure, while the double-story isolation structure shows the smallest floor shear. The double-story isolation structure showcases superior control over floor shear and excellent damping capability. However, when considering SSI on soft soil, the mid-story isolation structure demonstrates poor ability to control floor shear, with higher floor shear compared to the base-fixed structure in the Kern County wave and Whittier Narrows wave. Nevertheless, the double-story isolation structure still exhibits the lowest base shear.

### *4.5. Comparison of Maximum Acceleration of the Top Layer*

The maximum acceleration of the top layer of the structure is displayed in Figure 13. When SSI is not considered and when SSI is considered on hard soil, the maximum acceleration of the top floor of the mid-story isolation structure is lower than that of the base-fixed structure, while the maximum acceleration of the top floor of the double-story isolation structure is the smallest. This indicates that the double-story isolation structure effectively controls the maximum acceleration of the top floor, reducing the risk of structural damage. However, when SSI is considered on soft soil, there is a significant difference in the maximum acceleration of the top layer. The double-story isolation structure shows the lowest maximum acceleration at the top floor under the Kern County and Chi-Chi Taiwan waves, whereas under the Whittier Narrows wave, the maximum acceleration of the top floor of the double-story isolation structure is higher than that of the mid-story isolation structure.

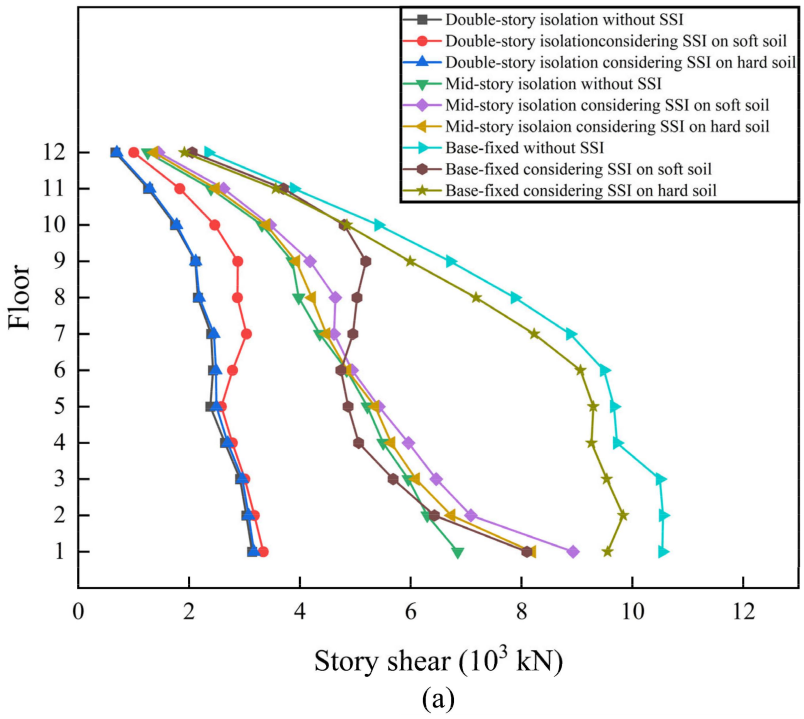


**Figure 12.** *Cont.*

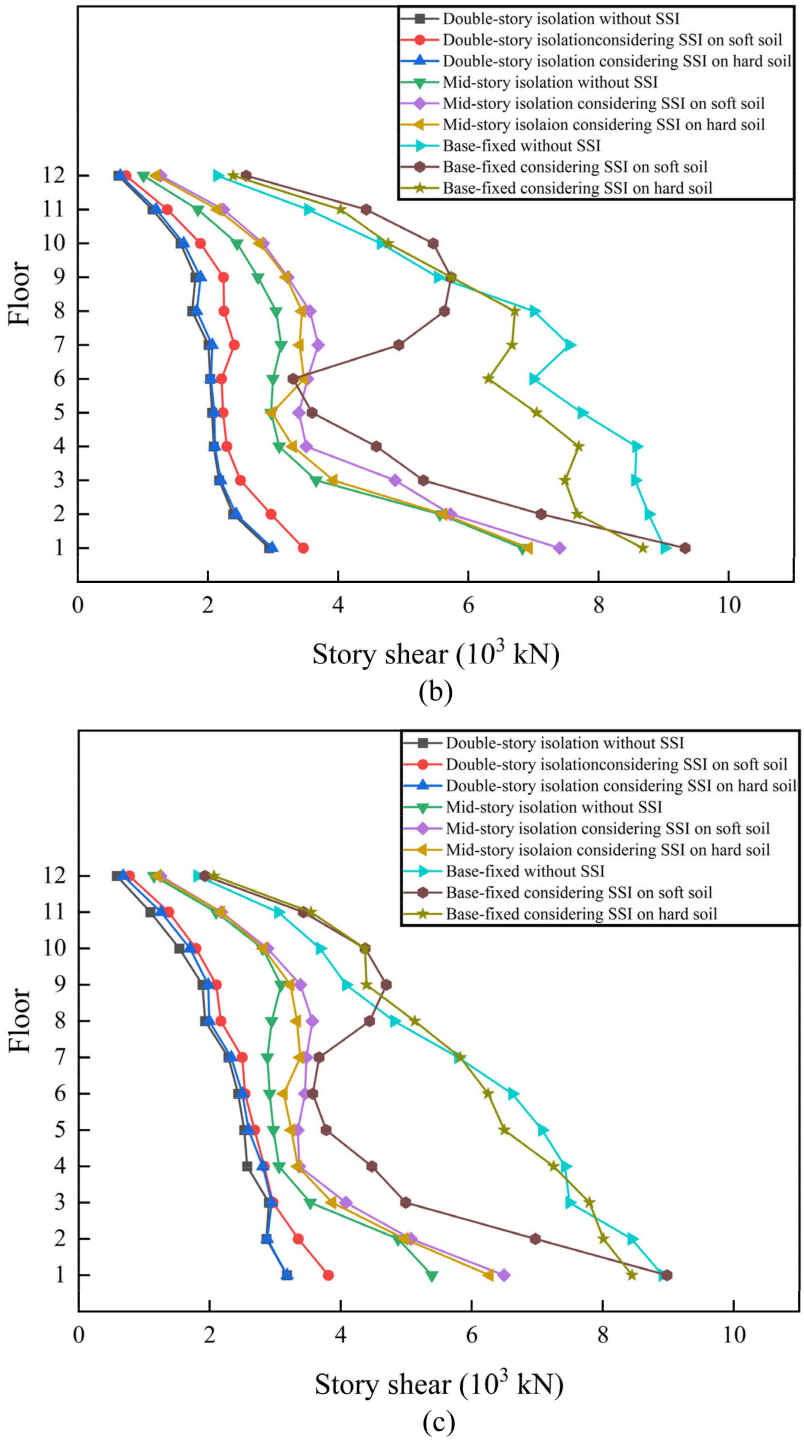


**Figure 12.** Story shear of the structure. (**a**) Story shear under the action of Kern County wave; (**b**) Story shear under the action of Whittier Narrows wave; (**c**) Story shear under the action of Chi-Chi wave.

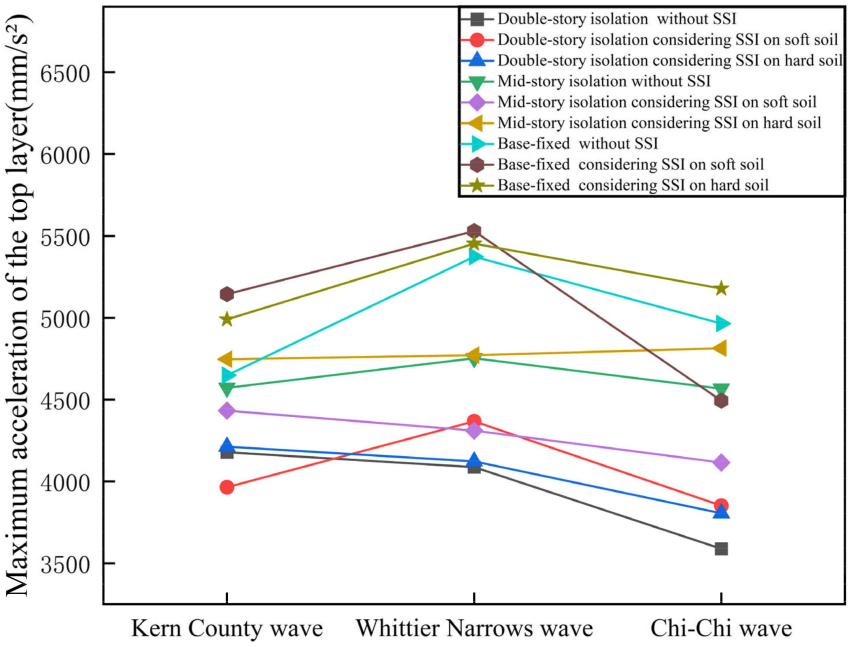


**Figure 13.** Maximum acceleration of the top layer.

### *4.6. Comparison of Overturning Moment*

According to the Code for Seismic Design of Buildings [26], the overturning moment of the structure is calculated as follows:

$$M_c = \sum_{i=1}^{n} \sum_{j=1}^{m} V_{ij} h_i$$

where $M_c$ is the seismic overturning moment under the horizontal force, $n$ is the number of stories of the structure, $m$ is the number of frame columns at the $i$ layer, $V_{ij}$ is the calculated seismic shear of the $j$-th frame column at the $i$ layer, and $h_i$ is the floor height at the $i$ layer.

The calculated anti-overturning moment of the structure is 533,162 kN·m and the overturning moments of the structure are shown in Table 9. None of the structures are at risk of overturning. The base-fixed structure exhibits the highest overturning moment, which is subsequently reduced after implementing seismic isolation. Notably, the double-story isolation structure demonstrates a significant reduction in overturning moment compared to the mid-story isolation structure. The reduction amounts to 42.5% when SSI is not considered, 40.9% when SSI is considered in soft soils, and 44.8% when SSI is considered in hard soils. These results highlight the excellent overturning resistance of the double-story isolation structure and significantly mitigate the risk of overturning damage to the overall structure.

**Table 9.** Overturning moment (kN·m).

| Structure Type | | Kern County Wave | Whittier Narrows Wave | Chi-Chi Wave |
|---|---|---|---|---|
| Double-story isolation structure | Without SSI | 88,746 | 74,537 | 85,087 |
| | Considering SSI on soft soil | 104,771 | 87,565 | 95,315 |
| | Considering SSI on hard soil | 90,396 | 76,272 | 88,545 |
| Mid-story isolation structure | Without SSI | 177,595 | 129,780 | 124,418 |
| | Considering SSI on soft soil | 197,218 | 149,348 | 140,366 |
| | Considering SSI on hard soil | 187,215 | 139,980 | 135,193 |
| Base-fixed structure | Without SSI | 315,347 | 264,147 | 228,241 |
| | Considering SSI on soft soil | 199,998 | 204,606 | 182,461 |
| | Considering SSI on hard soil | 291,180 | 248,047 | 229,553 |

## 5. Analysis of the Isolation Layer of the Double-Story Isolation System with SSI

### *5.1. Comparison of Displacement of the Isolation Layer*

The displacements of the isolation layers for the double-story isolation structure and the mid-story isolation structure are presented in Table 10. According to the Code for Seismic Design of Buildings [26], the ultimate displacement requirement for the isolation bearing HRB600 is 330 mm, and the displacements of the isolation layers in this study comply with the code requirements.

**Table 10.** Isolation layer displacement (mm).

| Type of Ground Motion | | | Without SSI | Considering SSI on Soft Soil | Considering SSI on Hard Soil |
|---|---|---|---|---|---|
| Kern County wave | Double-story isolation | Base isolation layer | 75.90 | 77.30 | 76.04 |
| | | Upper isolation layer | 50.82 | 62.49 | 46.56 |
| | Mid-story isolation | Upper isolation layer | 159.96 | 187.88 | 164.41 |
| Whittier Narrows wave | Double-story isolation | Base isolation layer | 73.58 | 77.04 | 73.97 |
| | | Upper isolation layer | 49.05 | 54.51 | 52.24 |
| | Mid-story isolation | Upper isolation layer | 83.10 | 86.68 | 85.64 |
| Chi-Chi wave | Double-story isolation | Base isolation layer | 68.83 | 99.84 | 71.81 |
| | | Upper isolation layer | 45.40 | 79.90 | 50.35 |
| | Mid-story isolation | Upper isolation layer | 61.23 | 88.25 | 61.88 |

Considering SSI, the displacement of the isolation layer in the double-story isolation structure increases. Among these, the displacement of the isolation layer beneath the soft ground foundation is the largest. In comparison, the displacement of the upper isolation layer in the double-story isolation structure is smaller than that in the mid-story isolation structure. This difference can be attributed to the dissipation of some earthquake energy in the base isolation layer, resulting in a displacement reduction in the upper isolation layer of the double-story isolation structure. This indicates that the double-story isolation structure effectively controls the displacement of the isolation layer, reducing the potential for damage to the isolation bearing.

### *5.2. Comparison of Tensile and Compressive Stresses of the Isolation Bearings*

To ensure the normal operation of the isolation bearings during rare earthquakes, the tensile and compressive stresses of the isolation bearings need to be calibrated. According to the Code for Seismic Design of Buildings [26], the tensile stress in the isolation bearings should not exceed 1 MPa and the compressive stress should not exceed 30 MPa. The tensile and compressive stresses of all isolation bearings did not exceed the standard limit values.

The tensile and compressive stresses in the isolation bearings for the double-story isolation structure and the mid-story isolation structure are depicted in Figures 14 and 15. It was observed that the tensile stresses in both the double-story isolation structure and the mid-story isolation structure were negative, indicating that no tensile stresses were generated in the isolation bearings.

Furthermore, the compressive stresses in the upper layer of the double-story isolation structure were lower than those in the upper layer of the mid-story isolation structure under three different soil conditions. This indicates that the double-story isolation system effectively reduces the compressive stresses experienced by the isolation bearing, thereby enhancing its stability. Additionally, the compressive stresses of the isolation bearings in the upper isolation layer of the double-story isolation structure were lower than those in the isolation bearings of the base isolation layer. The variation in compressive stress in isolation bearings becomes more complex when different soils are used in the double-story isolation structure. Moreover, significant differences are observed in the compressive stresses within

the isolation bearings at various locations. It is crucial to acknowledge the substantial influence of the soil on the overall structural behavior.

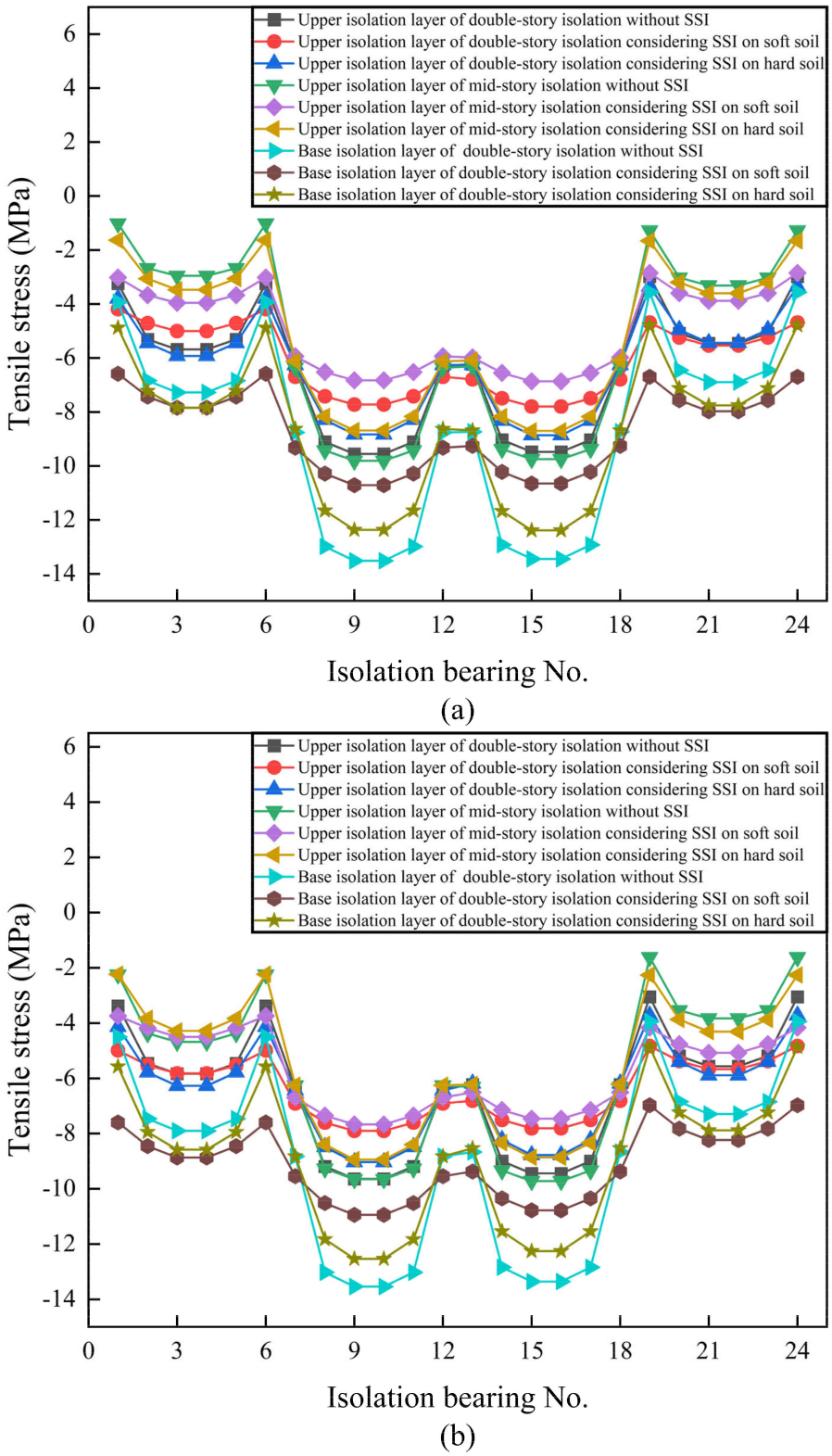


**Figure 14.** *Cont.*

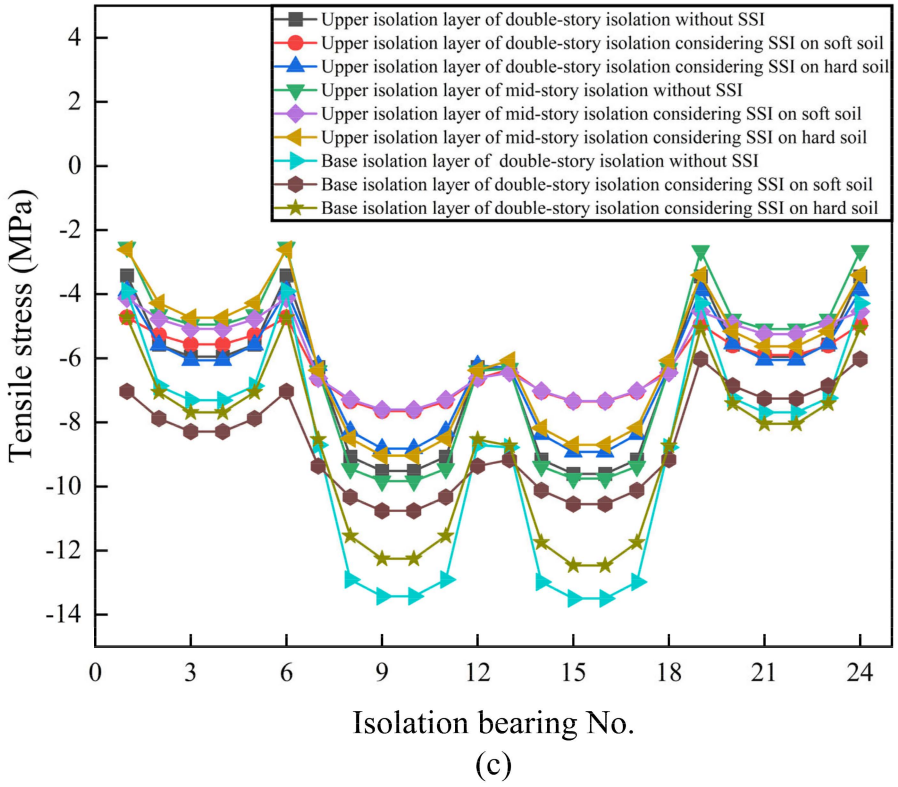


**Figure 14.** Tensile stresses of the isolation bearings. (**a**) Tensile stress of the isolation bearing under the action of Kern County wave; (**b**) Tensile stress of the isolation bearing under the action of Whittier Narrows wave; (**c**) Tensile stress of the isolation bearing under the action of Chi-Chi wave.

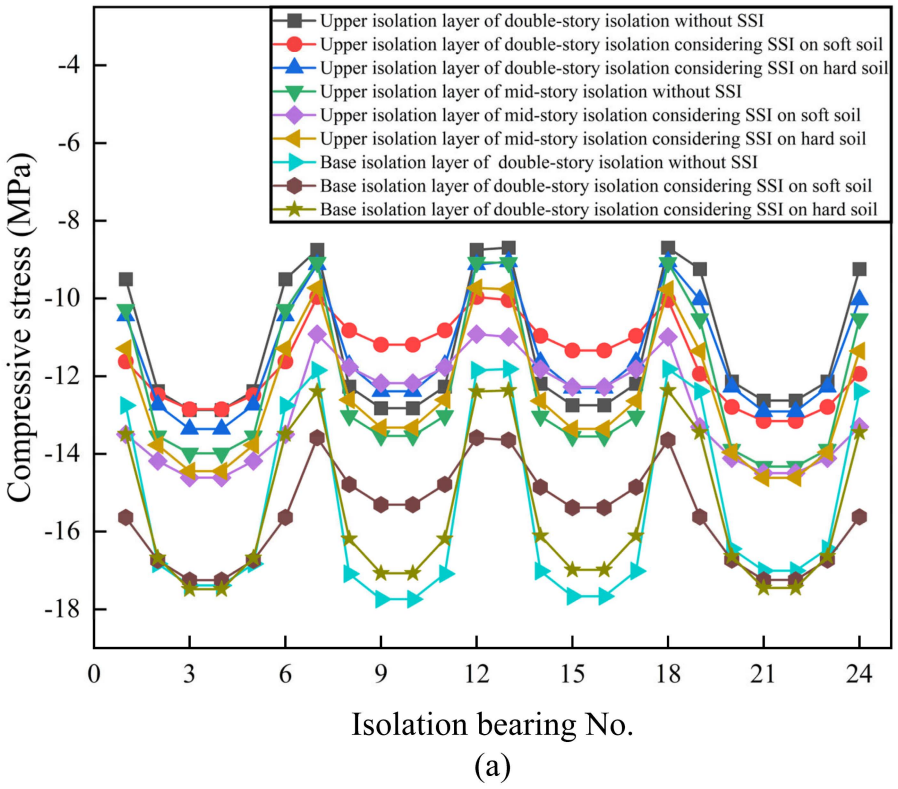


**Figure 15.** *Cont.*

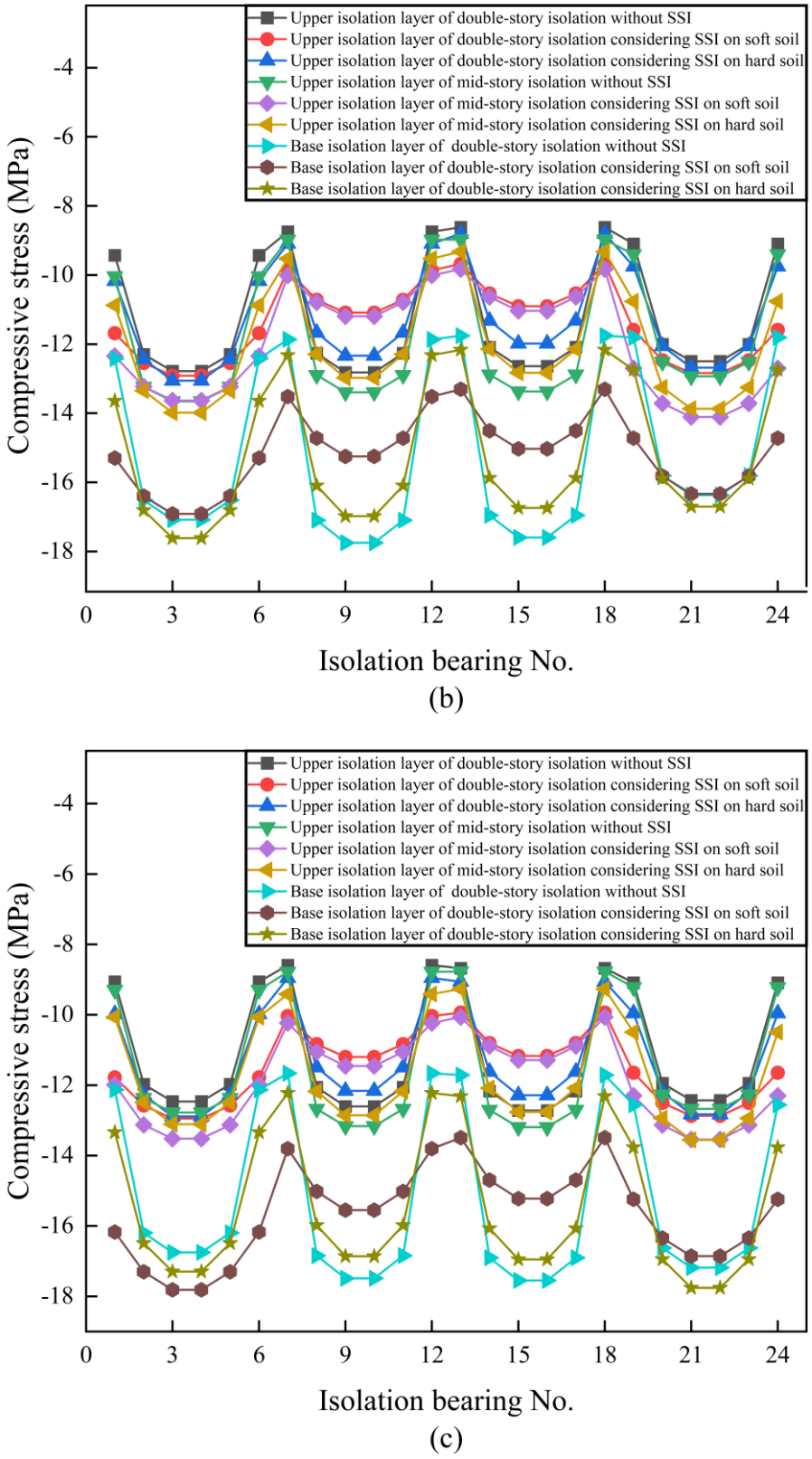


**Figure 15.** Compressive stresses of the isolation bearings. **(a)** Compressive stress of the isolation bearing under the action of Kern County wave; (**b**) Compressive stress of the isolation bearing under the action of Whittier Narrows wave; (**c**) Compressive stress of the isolation bearing under the action of Chi-Chi wave.

## 6. Structural Damage of the Double-Story Isolation System

### *6.1. Comparison of Structural Plastic Hinges*

The plastic hinges formed in the structure under the influence of different soil types are depicted in Figures 16–18. It is evident that the base-fixed structure generates the highest number of plastic hinges, while the double-story isolation structure exhibits the lowest count. This suggests that double-story isolation structures exert a significant attenuating effect on seismic forces compared to mid-story isolation structures. Additionally, when considering SSI on soft soil, double-story isolation structures exhibit the highest number of plastic hinges, whereas they show the lowest number of plastic hinges when SSI is not considered. This indicates that the influence of soft ground is more detrimental to the structure.

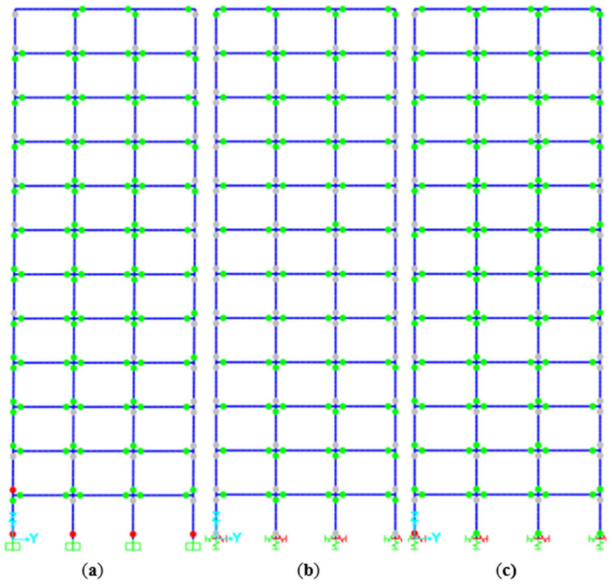


**Figure 16.** Plastic hinges of the base-fixed structure. (**a**) Without SSI; (**b**) Considering SSI on soft soil; (**c**) Considering SSI on hard soil.

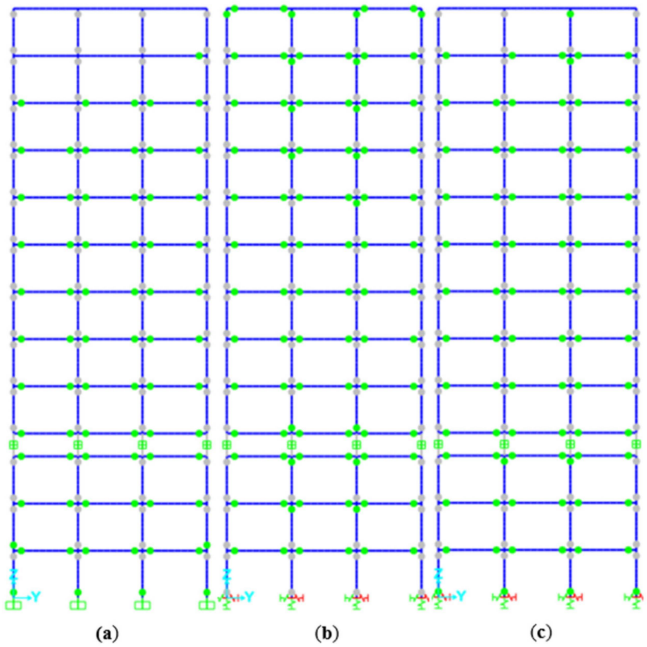


**Figure 17.** Plastic hinges of the mid-story isolation structure. (**a**) Without SSI; (**b**) Considering SSI on soft soil; (**c**) Considering SSI on hard soil.

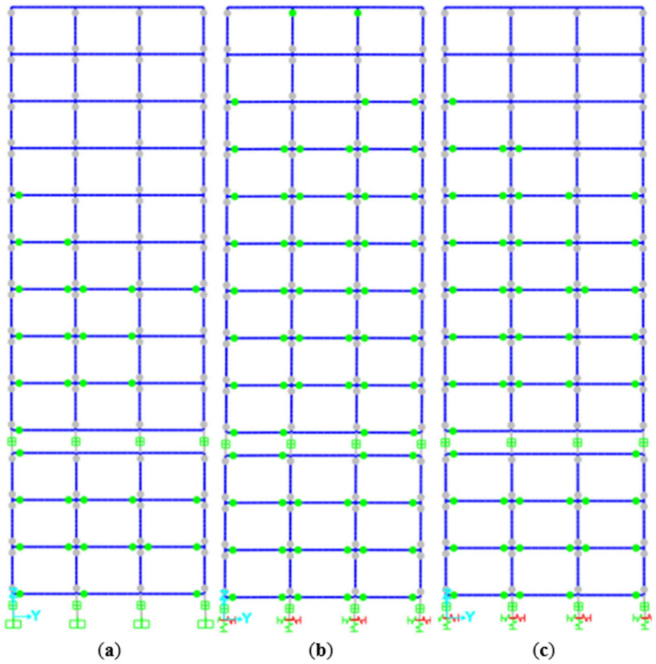


**Figure 18.** Plastic hinges of the double-story isolation structure. (**a**) Without SSI; (**b**) Considering SSI on soft soil; (**c**) Considering SSI on hard soil.

### *6.2. Comparison of Frame Stress Damage*

The frame damages of the structure under the influence of different soil types are depicted in Figures 19–21. Among the structures, the fixed foundation structure exhibits the highest level of stress damage. The mid-story isolation structure shows a decrease in stress damage, while the double-story isolation structure experiences the least amount of stress damage. This indicates that the double-story isolation structure effectively reduces seismic action, resulting in minimal damage to the structure.

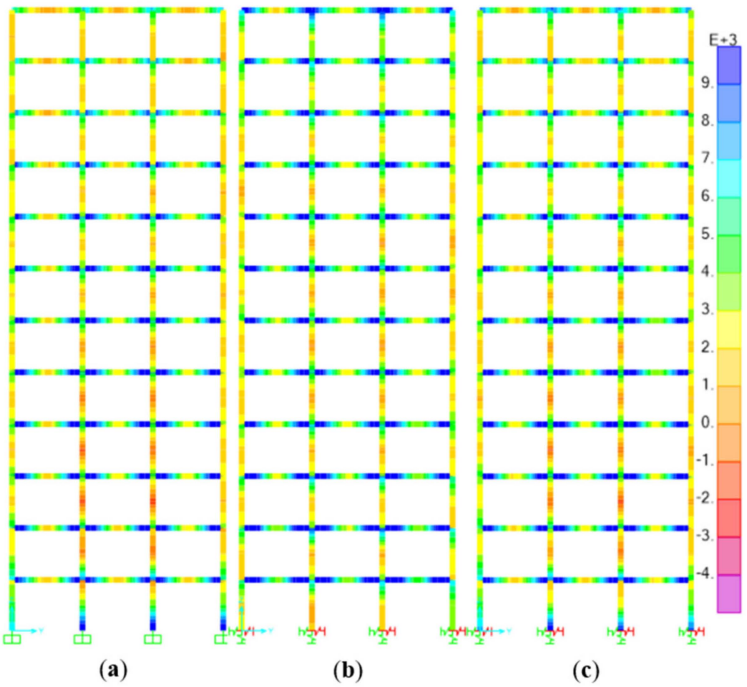


**Figure 19.** Frame damage of the base-fixed structure. (**a**) Without SSI; (**b**) Considering SSI on soft soil; (**c**) Considering SSI on hard soil.

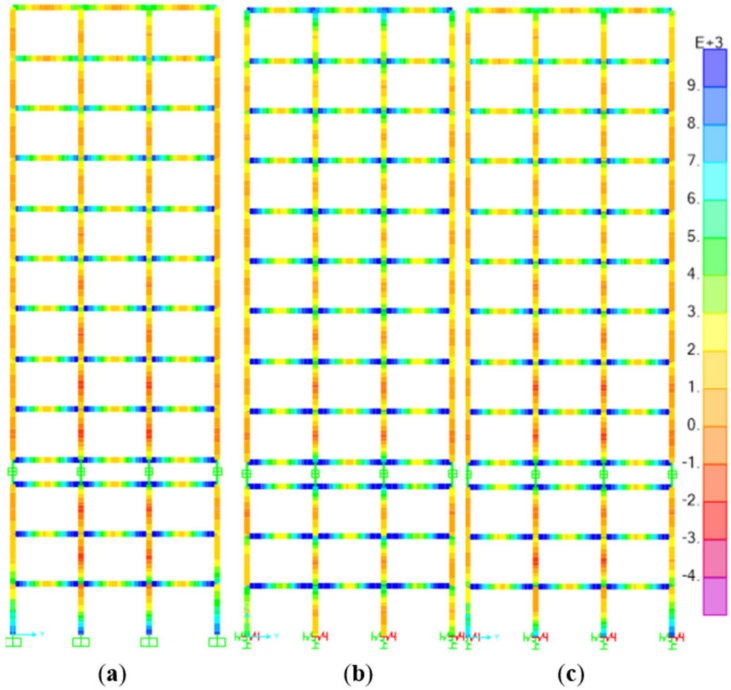


**Figure 20.** Frame damage of the mid-story isolation structure. (**a**) Without SSI; (**b**) Considering SSI on soft soil; (**c**) Considering SSI on hard soil.

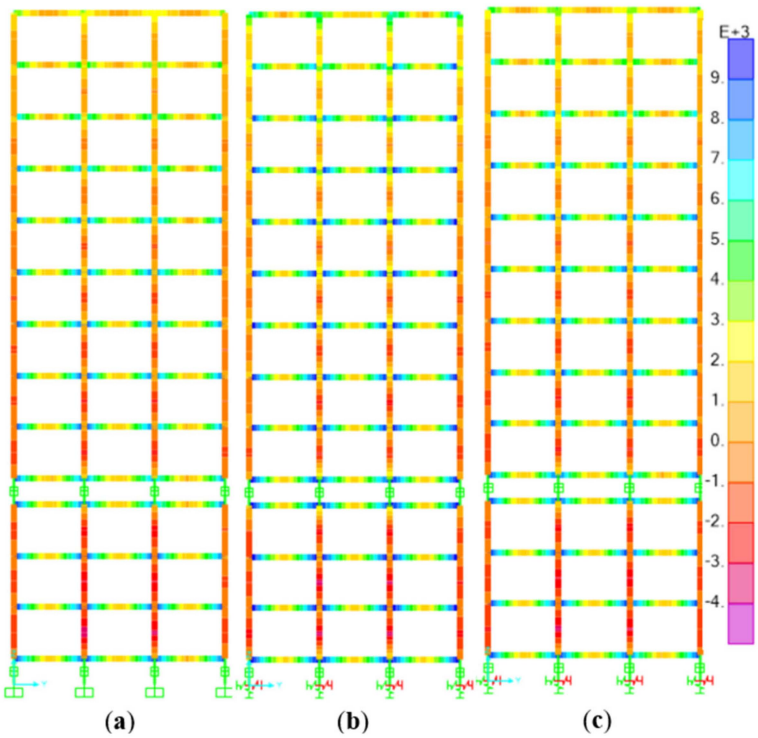


**Figure 21.** Frame damage of the double-story isolation structure. (**a**) Without SSI; (**b**) Considering SSI on soft soil; (**c**) Considering SSI on hard soil.

As the number of floors increases, the stress damage gradually decreases, with the bottom floor experiencing the greatest level of stress damage. When SSI is not considered, the stress damage of the double-story isolation structure is minimized. When considering SSI, stress damage increases, and it is most pronounced in soft ground. Soft soil has a more

intricate impact on structures, making them more susceptible to resonance. It should be paid more to attention during the design process.

## 7. Discussions

1. The double-story isolation structure, when not accounting for the SSI effect, demonstrates the ability to extend structural periods, resulting in reduced base shear, inter-story displacement, and maximum acceleration of the top layer compared to a base isolation structure. These findings are consistent with the results obtained by other scholars [24,25].
2. This paper focuses on the damping effectiveness of double-story isolation structures, considering the SSI effect. Double-story isolation structures demonstrate excellent damping effectiveness in hard soil conditions. However, in the case of soft soil, the damping capacity of the double-story isolation structure is poor. Additionally, when designing building projects in soft soil areas, it is essential to consider the potential drawbacks to the building structure, and accordingly, reinforce the construction of the structure.
3. This study analyzes the impact of SSI on the three structures, but it remains somewhat insufficient. Deep learning, artificial neural networks, and artificial intelligence have demonstrated significant importance in solving practical engineering problems [29–34]. In our upcoming research, we will undertake a comprehensive investigation into the application of deep learning, artificial neural networks, and artificial intelligence in the field of civil engineering. Our goal is to provide valuable insights for the future development of high-performance building structures.

## 8. Conclusions

In this paper, the models of the base-fixed structure, mid-story isolation structure, and double-story isolation structure were established, an elastoplastic analysis considering SSI under rare earthquakes was carried out, and the main conclusions are listed as follows:

1. The double-story isolation structure can prolong the structural period further than the base isolation structure, and the structural period increases as the soil softens and the structure becomes more flexible.
2. When considering SSI on hard soil and when SSI is not considered, the double-story isolation structure exhibits smaller base shear, story force, inter-story displacement, maximum acceleration of the top floor, and displacement of the isolation layer compared to the mid-story isolation structure. Conversely, the base-fixed structure shows the largest values for base shear, story force, inter-story displacement, and maximum acceleration of the top layer, indicating the significant shock-absorbing effect of the double-story isolation structure. However, when considering SSI on soft soil, the shock-absorbing effect of the isolation structure is diminished, and the effectiveness of the double-story isolation structure may not necessarily surpass that of the mid-story isolation structure.
3. In all three soil conditions, the compressive stresses generated in the isolation bearings of the upper layer of the double-story isolation structure are lower compared to those in the mid-story isolation structure, indicating better stability of the isolation bearings in the double-layer structure. However, the compressive stresses in the isolation bearings of the base isolation layer in the double-story isolation structure are higher than those in the upper isolation layer. Furthermore, the compressive stresses in the isolation bearings of the double-story isolation structure exhibit significant variations under different soil conditions, indicating the complex influence of soil on the structure.
4. In all three soil conditions, the double-story isolation structure exhibits significantly lower overall overturning moments compared to the mid-story isolation structure, demonstrating its excellent overturning resistance and superior overall structural

stability. It is worth noting that the highest overturning moment occurs when the foundation is composed of soft soil.

5. In all three soil conditions, double-story isolation structures exhibit fewer plastic hinges and lower stress damage to the frame compared to mid-story isolation structures, effectively mitigating seismic effects. However, double-story isolation structures experience the highest number of plastic hinges and the most frame stress damage when constructed on soft ground. Soft soil has a more intricate impact on structures, making them more susceptible to resonance. This aspect should receive greater attention in the design process.

**Author Contributions:** Conceptualization, D.L.; methodology, L.G.; software, S.M.; validation, Y.D.; formal analysis, L.G.; investigation, M.L.; resources, Y.D.; data curation, L.G.; writing—original draft preparation, L.G.; writing—review and editing, L.G., D.L., M.L., Y.D. and S.M.; visualization, S.M.; supervision, M.L.; project administration, D.L.; funding acquisition, D.L. All authors have read and agreed to the published version of the manuscript.

**Funding:** This research was funded by the National Natural Science Foundation of China, grant number (52168072, 51808467), and the High-level Talent Support Project of Yunnan Province, China (2020).

**Data Availability Statement:** The datasets used and/or analyzed during the current study are available from the corresponding author upon reasonable request.

**Conflicts of Interest:** The authors declare that there is no conflict of interest regarding the publication of this paper.

## References

1. Chai, W.C. *Mega-Sub Control of High-Rise Building*; University of California: Irvine, CA, USA, 1996.
2. Ou, J.P.; Wu, P.S.; Guan, X.C. Seismic resilient base isolated structure equipped with super-large displacement friction pendulum bearing and isolated structure equipped with multi-super-large displacement friction pendulum bearing. *J. Disaster Prev. Mitig. Eng.* **2021**, *41*, 657–676.
3. Loh, C.H.; Weng, J.H.; Chen, C.H.; Lu, K.C. System identification of mid-story isolation building using both ambient and earthquake response data. *Struct. Control Health Monit.* **2013**, *20*, 139–155. [CrossRef]
4. Zhou, Q.; Singh, M.P.; Huang, X.Y. Model reduction and optimal parameters of mid-story isolation systems. *Eng. Struct.* **2016**, *124*, 36–48. [CrossRef]
5. Takewaki, I.; Kanamori, M.; Yoshitomia, S.; Tsuji, M. New experimental system for base-isolated structures with various dampers and limit aspect ratio. *Earthq. Struct.* **2013**, *5*, 461–475. [CrossRef]
6. Eem, S.H.; Jung, H.J. Seismic response distribution estimation for isolated structures using stochastic response database. *Earthq. Struct.* **2015**, *9*, 937. [CrossRef]
7. Eem, S.H.; Jung, H.J. Seismic fragility assessment of isolated structures by using stochastic response database. *Earthq. Struct.* **2018**, *14*, 389–398.
8. Fallahian, M.; Khoshnoudian, F.; Loghman, V. Torsionally seismic behavior of triple concave friction pendulum bearing. *Adv. Struct. Eng.* **2015**, *18*, 2151–2166. [CrossRef]
9. Yang, W.; Bao, C.; Ma, X.; Zhang, S. Study on structural robustness of isolated structure based on seismic response. *Appl. Sci.* **2018**, *8*, 1686. [CrossRef]
10. Zhu, Y.H.; Lu, X.L.; Shi, W.X.; Feng, D.M. Analysis of the Seismic Response of the Building Models with Lead Rubber Bearings for Vibration Isolation. *J. Vib. Eng.* **2003**, 124–128. [CrossRef]
11. Wu, X.X.; Li, H.N. Effect of Vertical Motion on Limit Ratio of Height to Width for Isolated Structure. *J. Tongji Univ. (Nat. Sci.)* **2004**, *32*, 10–14.
12. Pan, Y.; Bao, Y.L.; Liu, Y.X.; Hu, S.Y. Seismic fragility analysis of base-isolation structure connected with large span special-shaped steel corridor. *China Civ. Eng. J.* **2021**, *54*, 20–29.
13. Zhang, Y.; Tan, P.; Zhou, F.L. Seismic response prediction for a story-isolation structure based on energy balance method. *J. Vib. Shock.* **2009**, *28*, 137–141+209.
14. Shi, C.; Du, Y. Evaluation of the collapse mode of isolated structures subjected to multi-directional dynamic coupling excitation based on reliability theory. *Structures* **2021**, *34*, 1261–1275. [CrossRef]
15. Wang, N.; Huang, X. Global damage model for the seismic reliability analysis of a base-isolated structure. *Structures* **2021**, *34*, 4892–4907. [CrossRef]
16. Karabork, T.; Deneme, I.O.; Bilgehan, R.P. A comparison of the effect of SSI on base isolation systems and fixed-base structures for soft soil. *Geomech. Eng.* **2014**, *7*, 87–103. [CrossRef]

17. Ashiquzzaman, M.; Hong, K.J. Simplified Model of Soil-Structure Interaction for Seismically Isolated Containment Buildings in Nuclear Power Plant. *Structures* **2017**, *10*, 209–218. [CrossRef]
18. Shourestani, S.; Soltani, F.; Ghasemi, M.; Etedali, S. SSI effects on seismic behavior of smart base-isolated structures. *Geomech. Eng.* **2018**, *14*, 161–174.
19. Krishnamoorthy, A. Effect of soil-structure interaction for a building isolated with FPS. *Earthq. Struct.* **2013**, *4*, 285–297. [CrossRef]
20. Zhang, Z.; Wei, H.; Qin, X. Experimental study on damping characteristics of soil-structure interaction system based on shaking table test. *Soil Dyn. Earthq. Eng.* **2017**, *98*, 183–190. [CrossRef]
21. Liu, S.; Lu, Z.; Li, P.; Ding, S.; Wan, F. Shaking table test and numerical simulation of eddy-current tuned mass damper for structural seismic control considering soil-structure interaction. *Eng. Struct.* **2020**, *212*, 110531. [CrossRef]
22. Dong, H.; Li, C.; Wen, J.; Han, Q.; Du, X. Seismic performance of self-centering rocking bents considering soil-structure interaction. *Soil Dyn. Earthq. Eng.* **2023**, *168*, 107845. [CrossRef]
23. Zhang, Y.; Tan, P.; Zhou, F.L. Study on seismic reduction performance and parameter design of newly segmented isolation system. *China Civ. Eng. J.* **2010**, *43* (Suppl. S1), 270–275.
24. Rong, Q.; Lu, N.; Zhang, X.; Wang, G.K. Seismic response analysis of double isolation system in high-rise building. *Earthq. Resist. Eng. Retrofit.* **2018**, *40*, 87–92.
25. Rong, Q.; Wu, D.; Sheng, Y. Seismic response analysis of double isolation system subjected to near-fault ground motions. *Earthq. Resist. Eng. Retrofit.* **2021**, *43*, 54–61.
26. *GB 50011-2010 (2016)*; Code for Seismic Design of Buildings. China Architecture & Building Press: Beijing, China, 2016.
27. ATC. *The Seismic Evaluation and Retrofit of Concrete Buildings. Volume 1 and 2*; ATC-40 Report; Applied Technology Council: Redwood City, CA, USA, 1996.
28. Fema A 440. *Improvement of Nonlinear Static Seismic Analysis Procedures*; FEMA-440: Redwood City, CA, USA, 2005; Volume 7, p. 11.
29. Hu, X.; Kuang, Q.; Cai, Q.; Xue, Y.; Zhou, W.; Li, Y.A. Coherent Pattern Mining Algorithm Based on All Contiguous Column Bicluster. *J. Artif. Intell. Technol.* **2022**, *2*, 80–92. [CrossRef]
30. Du, H.; Du, S.; Li, W. Probabilistic time series forecasting with deep non-linear state space models. *CAAI Trans. Intell. Technol.* **2023**, *8*, 3–13. [CrossRef]
31. Zhang, Z.; De Luca, G.; Archambault, B.; Chavez, J.; Rice, B. Traffic Dataset and Dynamic Routing Algorithm in Traffic Simulation. *J. Artif. Intell. Technol.* **2022**, *2*, 111–122. [CrossRef]
32. Zhao, H.; Ma, L. Several rough set models in quotient space. *CAAI Trans. Intell. Technol.* **2022**, *7*, 69–80. [CrossRef]
33. Hsiao, I.H.; Chung, C.Y. AI-infused semantic model to enrich and expand programming question generation. *J. Artif. Intell. Technol.* **2022**, *2*, 47–54. [CrossRef]
34. Chen, J.; Yu, S.; Wei, W.; Ma, Y. Matrix-based method for solving decision domains of neighbourhood multigranulation decision-theoretic rough sets. *CAAI Trans. Intell. Technol.* **2022**, *7*, 313–327. [CrossRef]